

Low-voltage ZnO varistor fabricated by the solution-coating method

Q. Wang^a, Y. Qin^{a,*}, G.J. Xu^b, L. Chen^a, Y. Li^{a,b}, L. Duan^b, Z.X. Li^b, Y.L. Li^b, P. Cui^b

^a Key Laboratory of Materials Physics, Institute of Solid State Physics, Chinese Academy of Sciences, PO Box 1129, Hefei 230031, PR China

^b Ningbo Institute of Material Technology & Engineering, Chinese Academy of Sciences, Ningbo 315040, PR China

Received 26 February 2007; received in revised form 28 March 2007; accepted 12 May 2007

Available online 10 August 2007

Abstract

A novel solution nano-coating technique, by coating ZnO powder with a mixed solution of dopants, has been developed to produce high performance low-voltage ZnO varistors. The sintering temperature in the present route is about 50 °C lower than that in the conventional oxide mixing route. The microstructure and electrical characteristics were examined by XRD, SEM and dc power supply and the results showed that the specimens prepared by the solution-coating route have bigger grain sizes, more evenly distributed intergranular phases, higher densities and nonlinearity coefficients, lower breakdown fields and leakage currents than those from the conventional oxide mixing route. The improved current–voltage properties are attributed to the excellent performance of the nano-composite ZnO powder and the advantages of the solution nano-coating technique.

© 2007 Elsevier Ltd and Techna Group S.r.l. All rights reserved.

Keywords: C. Electrical properties; D. ZnO; E. Varistors; Microstructure

1. Introduction

Zinc oxide varistors, due to their highly nonlinear current–voltage characteristics and energy handling capabilities, have been widely used as surge absorbers in small current electronic circuits as well as large current transmission lines for over-voltage protection [1–4]. As the development of large scale integrated electronics, low-voltage varistors have attracted more and more attention [5,6]. Developing materials that exhibit high nonlinear current–voltage characteristics at lower voltage has become an important aspect in the academe and industry researches of the varistor.

Two principal approaches have been used for making low-voltage ZnO varistors. One approach is thinning the devices, such as multilayering, thin foil, and thick film techniques, etc. [7]. However the strength and energy absorption capabilities of the thin ZnO varistor are very poor due to its small volume. The other is the classical approach of optimizing the processing and composition of conventional varistor in order to maximize ZnO grain size [8]. In this approach even growth of ZnO grains is

requested in order to obtain a dense uniform ZnO varistor with large size grains.

The homogeneous starting powder is necessary for the manufacture of high performance ZnO varistors [9–11]. It is difficult for the conventional oxide mixing route to obtain homogeneous composite powder [9,12], so several chemical methods have been developed in the last decade, such as coprecipitation [13], sol–gel [3,11,14], microemulsion [15] and polymerized complex method [12]. However most of these methods are complicated and costly, or not suitable to the production of low-voltage ZnO varistors.

‘Solution-coating technique has been reported in preparation of high-voltage ZnO varistors recently [9,16], but not used in low-voltage ZnO varistors. In the present work, the low-voltage ZnO varistors were prepared by a novel solution nano-coating technique. The homogeneous nano-composite ZnO powders with few aggregates were obtained by coating ZnO powder with a mixed solution of dopants and the low-voltage ZnO varistors were successfully synthesized using these powders.

2. Experimental procedure

The ZnO mixed powders prepared in the present study contained 97.99% ZnO, 0.5% Bi₂O₃, 0.5% TiO₂, 0.5% MnO,

* Corresponding author. Tel.: +86 551 5591424; fax: +86 551 5591434.

E-mail address: yqin@issp.ac.cn (Y. Qin).

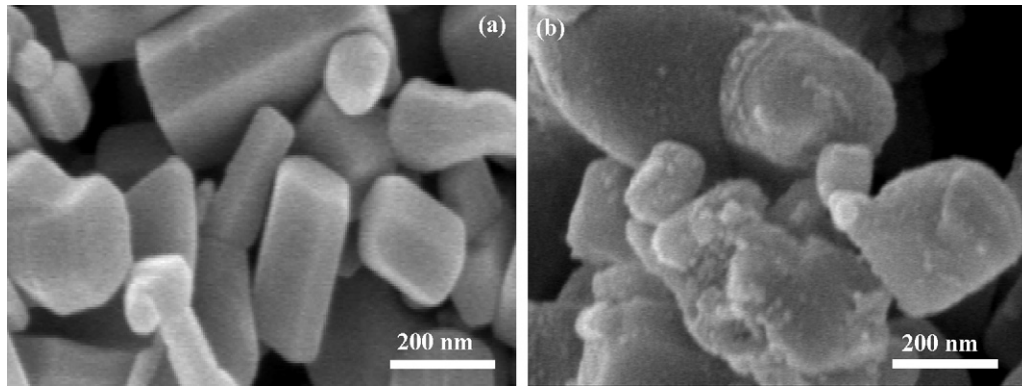


Fig. 1. The morphology of ZnO powder (a) before and (b) after nano-coating.

0.5% CoO and 0.01% Al₂O₃ (all compositions in mol%). For the solution-coating route, the starting materials for the production of ZnO varistor powder included ZnO (commercial), Bi(NO₃)₃·5H₂O (AR), Co(NO₃)₂·6H₂O (AR), Mn(NO₃)₂ (AR), Al(NO₃)₃·9H₂O (AR) and C₁₆H₃₆O₄Ti (CP). A mixed alcohol solution containing the required amounts of metal nitrates and C₁₆H₃₆O₄Ti was prepared. After stirring about 2 h, ZnO powder was added to the solution, and the mixture was kept in a water bath at about 80 °C with constant stirring until it changed into slurry. The slurry was dried at 150 °C for 8 h and ground into powder and then heated at 450 °C for 5 h to decompose nitrates. Thus, ZnO particles were covered with oxides of additives, resulting in the formation of nano-coated ZnO powders. The nano-composite ZnO powders were obtained by calcining at 750 °C for 2 h in air.

In the conventional oxide mixing route, varistor powder of the same effective composition was prepared by ball milling a mixture of oxides of dopants with ZnO powder in the required proportion. The milled powder was calcined at 450 °C for 5 h and 750 °C for 2 h in air.

Green compacts of mixed powder were made using uniaxial press at 200 MPa. Then green compacts were sintered at 1150, 1200, 1250 and 1280 °C for 2.5 h in air, respectively. Those sintered samples are labeled as sample A1150, A1200, A1250, A1280 for the solution-coating route and B1150, B1200, B1250, B1280 for the conventional oxide mixing route, respectively.

Phase formation of the powder and the sintered samples was characterized by means of X-ray diffraction (XRD) in a Philips X'Pert PRO X-ray diffractometer with Cu K α radiation. The microstructures of the powder and the sintered samples were examined by field emission scanning electron microscope (SEM, Sirion 200 FEG), in which the specimens were coated with gold for SEM observation. The elements present in the various phases were identified using EDS spot analysis. Density of the samples was determined by weight/geometric measurements.

Current–voltage response was measured using a dc power supply, a micro-ammeter and a voltmeter. The varistor voltage at 0.1 and 1 mA was measured for determining the threshold voltage and the nonlinearity coefficient α

evaluated in terms of relation:

$$\alpha = \frac{\log I_2 - \log I_1}{\log V_2 - \log V_1}$$

where V_2 and V_1 are the voltage corresponding to $I_2 = 1$ mA and $I_1 = 0.1$ mA, respectively. The leakage current (I_L) was measured at $0.75V_{1 \text{ mA}}$.

3. Results and discussion

Fig. 1 is SEM images showing the morphology of ZnO powder, in which Fig. 1(a) and (b) shows ZnO powder before and after nano-coating, respectively. The ZnO particle size ranges from 100 to 400 nm and the mean grain size is about 300 nm. The surface of the ZnO particles is smooth for Fig. 1(a) and rough for (b), indicating that ZnO particles were coated with the additives after nano-coating. It can be seen that the size of additives is much smaller compared with that of ZnO particles.

Fig. 2 shows the XRD patterns of the mixed powder and the sintered ZnO varistors from the solution-coating route. Besides

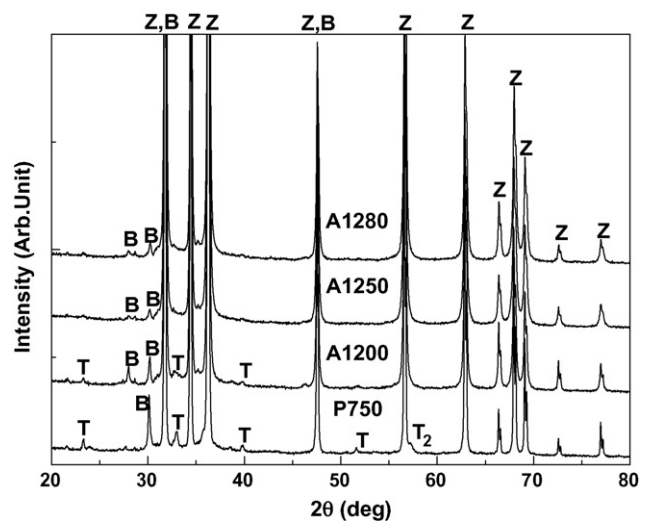


Fig. 2. XRD patterns of mixed powder P750 from the solution-coating route calcined at 750 °C and samples A1200, A1250 and A1280. Z-ZnO, S-Zn₂TiO₄, T-Bi₄Ti₃O₁₂, T₂-Bi₁₂Ti₂₀, B-Bi₂O₃.

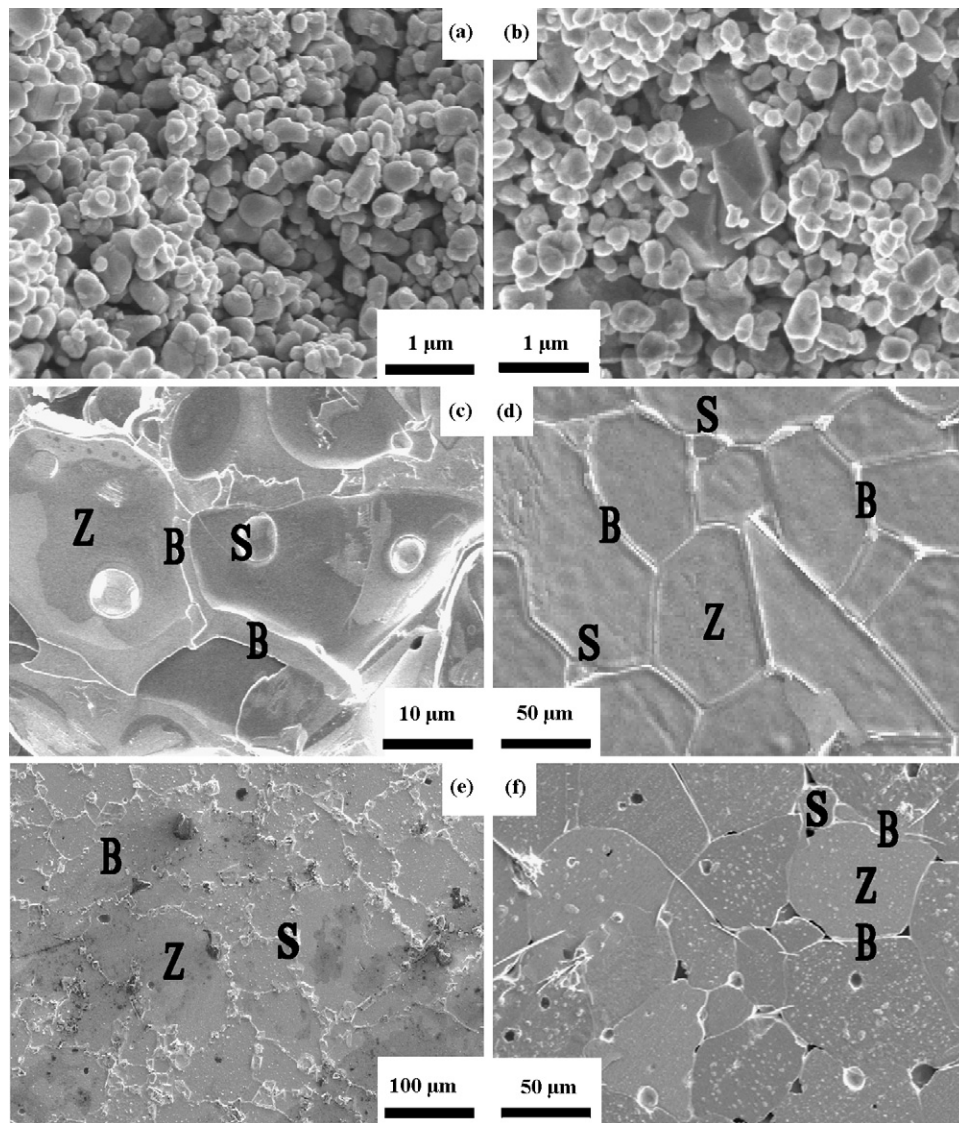


Fig. 3. SEM micrographs of different ZnO samples: (a) and (b) green sample (fracture) made from the solution-coating route and the conventional oxide mixing route, respectively, (c) A1200 (fracture), (d) A1250, (e) A1280 and (f) B1280 (thermal-etched surfaces). Z-ZnO, S-Zn₂TiO₄, B-Bi₂O₃.

ZnO phase and Bi₂O₃ phase, Bi₄Ti₃O₁₂ and Bi₁₂TiO₂₀ pyrochlore phases were observed at sample P750, suggesting that TiO₂ has reacted with the Bi₂O₃ at 750 °C.

With increasing sintering temperature the pyrochlore phase disappears, indicating that the Bi₄Ti₃O₁₂ and Bi₁₂TiO₂₀ reacted with the ZnO and formed Zn₂TiO₄ spinel phase [18,19], however, it is difficult to observe obvious increase of the content of Zn₂TiO₄ phase in sample A1250 and A1280 (see Fig. 2). One possible reason is that the Zn₂TiO₄ phase was covered with ZnO major phase, which may be confirmed by the result of SEM and EDS analysis.

The SEM images shown in Fig. 3 correspond to the green samples and the sintered samples of ZnO varistors prepared from the different routes. Fig. 3(a) and (b) shows the microstructure of green samples of ZnO varistors from solution-coating route and conventional oxide-mixing route, respectively. Compared with Fig. 3(b), the ZnO particles in Fig. 3(a) have a narrow size distribution and there are few

aggregates, indicating that the solution-coating route can obtain more homogeneous green samples than the conventional oxide-mixing route. The microstructures of sintered specimens are significantly dependent on the powder synthesis and sintering conditions. Fig. 3(c)–(e) shows the microstructure of sintered samples of ZnO varistors from solution-coating route whereas Fig. 3(f) represents the microstructure of sintered samples of ZnO varistors prepared by conventional oxide-mixing route. From Fig. 3(c)–(e) one can see that the ZnO grains grew stage by stage with increasing the sintering temperature and that some bismuth-rich, Zn₂TiO₄ spinel evenly distributed in the grain boundary. Sample A1280 has bigger and more homogeneous ZnO grains, more evenly distributed intergranular phases and more compact modality than sample B1280.

Results of EDS spot analysis of ZnO varistors are presented in Fig. 4. It can be determined from EDS spectra and SEM observations that the ZnO varistors are composed of ZnO, Bi₂O₃ and Zn₂TiO₄ phases. This result approved that the

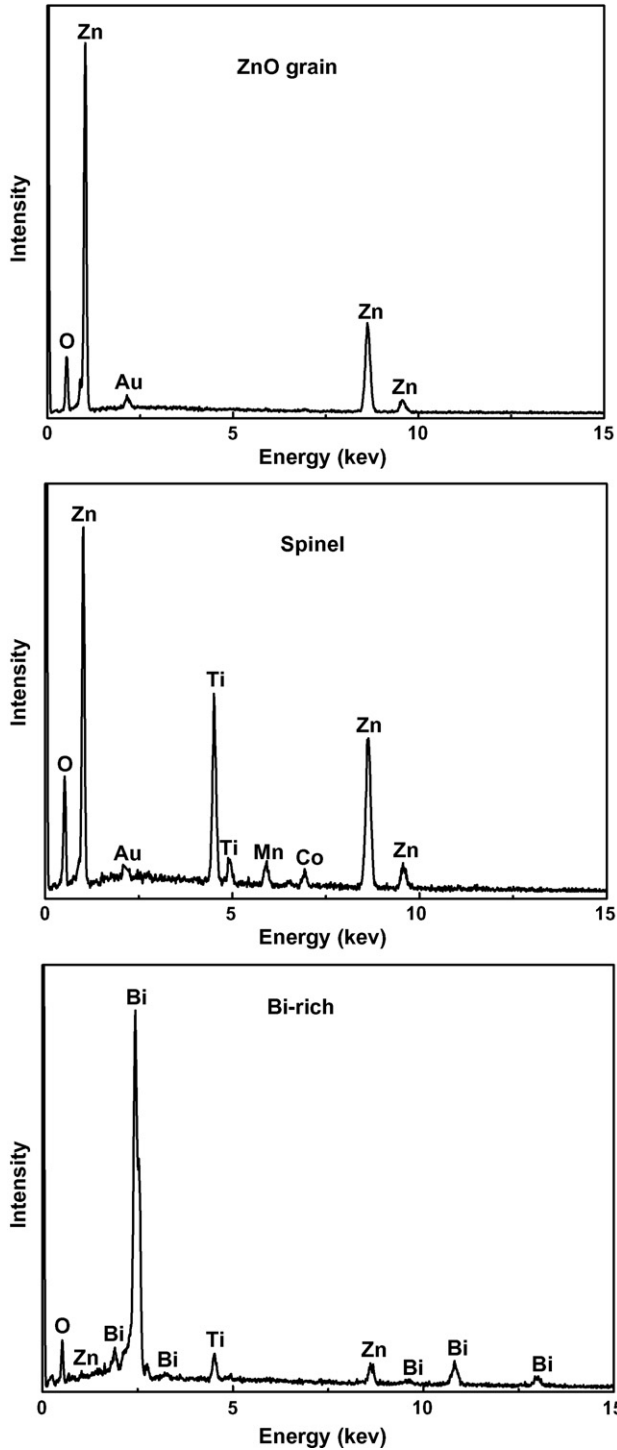


Fig. 4. EDS spectra of spot analysis of ZnO varistor prepared by solution-coating route.

Table 1
The characteristic parameters of the sintered ZnO varistors

Parameter	Sample							
	A1150	A1200	A1250	A1280	B1150	B1200	B1250	B1280
ρ (g/cm ³)	5.4 (4)	5.4 (2)	5.3 (4)	5.3 (3)	5.4 (1)	5.3 (9)	5.3 (2)	5.3 (2)
V_b (V/mm)	93.4 (9)	48.9 (7)	35.0 (1)	27.0 (1)	109.9 (1)	98.2 (2)	48.4 (5)	35.3 (7)
α	28.7 (7)	23.1 (0)	24.7 (7)	26.8 (1)	22.6 (6)	16.3 (6)	24.2 (8)	19.5 (8)
I_L (μ A)	26 (5)	17 (1)	12 (0)	12 (0)	36 (4)	43 (5)	23 (2)	35 (3)

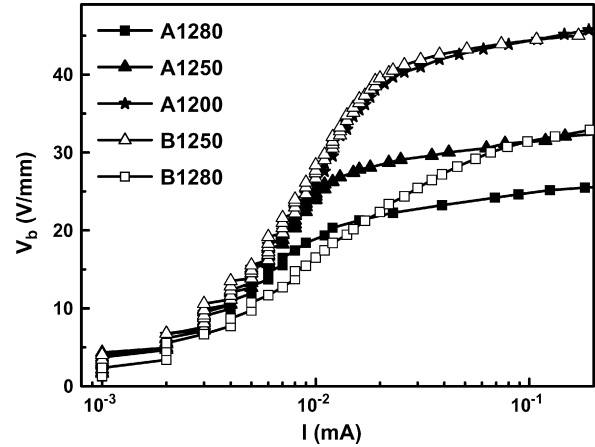


Fig. 5. The nonlinear I - V characteristics of sintered ZnO varistors.

Zn_2TiO_4 phases were covered with ZnO major phases so that they were unclearly in the XRD patterns. According to the EDS results the other dopants such as MnO and CoO are mostly located in the grain boundaries, which is consistent with the previous studies [4,9]. The Al_2O_3 is not detected by EDS due to very small content.

Table 1 summarizes the densities and electrical parameters of these sintered varistors, where ρ is the density, V_b the breakdown field, and I_L is the leakage current. The densities and breakdown fields of all sintered varistors decrease with increasing the sintering temperature. The density decreasing is related to the vaporization of Bi_2O_3 at high temperature [13,18,19], while the growth of ZnO grains at high temperature leads to the decrease of breakdown field. Furthermore, the A series varistors are associated with lower breakdown fields and leakage currents, higher nonlinearity coefficients and densities compared to the B series varistors, meaning that the solution-coating route is better in preparing low-voltage ZnO varistor compared to the oxide mixing route.

The nonlinear I - V characteristics of sintered ZnO varistors are showed in Fig. 5. Clearly, there is an obvious improvement in electrical properties for the A series varistors compared to the B series varistors. Due to the small size and the narrow size distribution of the composite nano-additives, all the dopants influencing the growth of grains can be in a position uniformly around the ZnO grains [17] and the growing rate of ZnO grains is similar. The homologous microstructures lead to the low breakdown fields, the large nonlinearity coefficients, and the diminished leakage currents.

In addition, owing to the effects of nanometer of the multiplex composite nano-additives, the surface-activity of the

obtained powders augments, which makes the mass transformation of liquid phase turn up more earlier than the conventional oxide mixing route during sintering process [17] and plays a dominant role in accelerating ZnO grain growth. So the solution-coating route can lower the sintering temperature of ZnO varistor ceramic by 50 °C or so.

4. Conclusions

Homogeneous nano-composite ZnO powders with few aggregates are prepared by a novel solution nano-coating technique. A series of low-voltage ZnO varistors with high performance are successfully synthesized using the as-prepared ZnO powders. The varistors prepared by the solution-coating route are associated with lower breakdown fields and leakage currents, higher nonlinearity coefficients and densities in contrast with the varistors prepared by the conventional oxide mixing route, suggesting that the novel solution nano-coating technique is more suitable for preparing low-voltage ZnO varistors.

Acknowledgment

The authors would like to thank Mr. M.G. Kong for his technical assistance in SEM characterization.

References

- [1] M. Inada, Formation mechanism of nonohmic zinc oxide ceramics, *Jpn. J. Appl. Phys.* 19 (1980) 409–419.
- [2] C.C. Zhang, Y.X. Hu, W.Z. Lu, M.H. Cao, D.X. Zhou, Influence of TiO₂/Sb₂O₃ ratio on ZnO varistor ceramics, *J. Eur. Ceram. Soc.* 22 (2002) 61–65.
- [3] J.C. Zhang, S.X. Cao, R.Y. Zhang, L.M. Yu, C. Jing, Effect of fabrication conditions on *I*–*V* properties for ZnO varistor with high concentration additives by sol–gel technique, *Curr. Appl. Phys.* 5 (2005) 381–386.
- [4] P. Durán, F. Capel, J. Tartaj, C. Moure, Low-temperature fully dense and electrical properties of doped-ZnO varistors by a polymerized complex method, *J. Eur. Ceram. Soc.* 22 (2002) 67–77.
- [5] M.H. Wang, K.A. Hu, B.Y. Zhao, N.F. Zhang, Electrical characteristics and stability of low voltage ZnO varistors doped with Al, *Mater. Chem. Phys.* 100 (2006) 142–146.
- [6] D.X. Zhou, C.C. Zhang, S.P. Gong, Degradation phenomena due to dc bias in low-voltage ZnO varistors, *Mater. Sci. Eng. B* 99 (2003) 412–415.
- [7] L.J. Bowen, F.J. Avella, Electrical properties and failure prediction in low-clamping voltage zinc oxide varistors, *J. Appl. Phys.* 54 (5) (1983) 2764–2772.
- [8] D.R. Clark, Varistor ceramics, *J. Am. Ceram. Soc.* 82 (3) (1999) 485–502.
- [9] A. Banerjee, T.R. Ramamohanb, M.J. Patnib, Smart technique for fabrication of zinc oxide varistor, *Mater. Res. Bull.* 36 (2001) 1259–1267.
- [10] D. Makovec, D. Kolar, M. Trontelj, Sintering and microstructural development of metal oxide varistor ceramics, *Mater. Res. Bull.* 28 (1993) 803–811.
- [11] X.Y. Kang, T.D. Wang, Y. Han, M.D. Tao, Sol–gel process doped ZnO nanopowders and their grain growth, *Mater. Res. Bull.* 32 (1997) 1165–1171.
- [12] P. Durán, F. Capel, J. Tartaj, C. Moure, A strategic two-stage low-temperature thermal processing leading to fully dense and fine-grained doped-ZnO varistors, *Adv. Mater.* 14 (2) (2002) 137–141.
- [13] H. Toplan, Y. Karakas, Processing and phase evolution in low voltage varistor prepared by chemical processing, *Ceram. Int.* 27 (2001) 761–765.
- [14] S.Y. Chu, T.M. Yan, S.L. Chen, Analysis of ZnO varistors prepared by the sol–gel method, *Ceram. Int.* 26 (2000) 733–737.
- [15] M. Singhal, V. Chhabra, P. Kang, D.O. Shah, Synthesis of ZnO nanoparticles for varistor application using Zn-substituted aerosol to micro-emulsion, *Mater. Res. Bull.* 32 (1997) 239–247.
- [16] Y.K. Li, G.R. Li, Q.R. Yin, Preparation of ZnO varistors by solution nano-coating technique, *Mater. Sci. Eng. B* 130 (2006) 264–268.
- [17] J.Z. Shi, Q.X. Cao, Y.G. Wei, Y.X. Huang, ZnO varistor manufactured by composite nano-additives, *Mater. Sci. Eng. B* 99 (2003) 344–347.
- [18] H. Suzuki, R.C. Bradt, Grain growth of ZnO in ZnO–Bi₂O₃ ceramics with TiO₂ additional, *J. Am. Ceram. Soc.* 78 (5) (1995) 1354–1360.
- [19] J. Wong, Sintering and varistor characteristics of ZnO–Bi₂O₃ ceramics, *J. Appl. Phys.* 51 (8) (1980) 4453–4459.